

Refined Fourier-transform method of analysis of full two-dimensional digitized interferograms

Davorin Lovrić, Zlatko Vučić, Jadranko Gladić, Nazif Demoli, Slobodan Mitrović, and Mirko Milas

A refined Fourier-transform method of analysis of interference patterns is presented. The refinements include a method of automatic background subtraction and a way of treating the problem of heterodyning. The method proves particularly useful for analysis of long sequences of interferograms. © 2003 Optical Society of America

OCIS codes: 100.2000, 100.2650, 100.5070.

1. Introduction

The motivation behind this work stems from the single crystal growth experiments performed in our laboratory and presented elsewhere.¹⁻³ We have investigated the growth of the equilibrium-like and well-faceted spherically shaped single crystals of mixed superionic conductors (cuprous and silver selenides) under the conditions of constant volume growth rate, constant temperature (approximately 800 K) and fixed stoichiometry. In Fig. 1(a) we show the cuprous selenide crystal growing on the capillary tip. The bright areas of the spherical single crystal correspond to the facets, the growth of which, in the direction perpendicular to the surface, has been monitored by means of the interferometric measurements⁴ in which the displacement of the facets due to the radial growth had been determined from the phase differences of two subsequent interferograms. In Fig. 1(b) we show a typical frame (320×240 pixels) recorded during the growth process. We have extracted (and analyzed) from each frame an area of 64×64 pixels (which we term interferogram throughout this paper) containing the fringe pattern. The frames have been taken by a CCD camera at the rate of 25 frames per second, because we wanted to access a wide range of growth rates. Our interferograms have been influenced by two kinds of perturbations, i.e., the mechanical vibrations and the

thermal fluctuations. The thermal fluctuations have been caused by thermal convection of air around the tubular furnace, heated by helicoidally wound wire, within which the quartz ampoule containing our capillary has been mounted, which may have changed the optical properties of various optically transparent elements situated on the optical path of laser beams. The mechanical perturbations have been caused by the antivibration table, by vibrations of the furnace itself, and are due to the other external sources of vibrations. All of them have manifested themselves at the tip of the long and narrow capillary where the crystal has grown. Because our crystals have usually grown for at least 72 h, we may use this fact to remove significantly, by means of other methods, the influence of perturbations happening on the time scale that is much longer than the time scale of the taking of the individual frame.³ However, we are still left with fast vibrations influencing each interferogram. One way of dealing with this problem has been our high frame-taking rate of 25 frames per s which diminishes the possibility that the value of the mean phase difference between two successive frames recorded exceeds π .

In a typical experiment we analyze as much as $6\frac{1}{2}$ million of interferograms. Wanting to analyze such a large amount of interferograms makes the use of an automatic method of analysis mandatory.

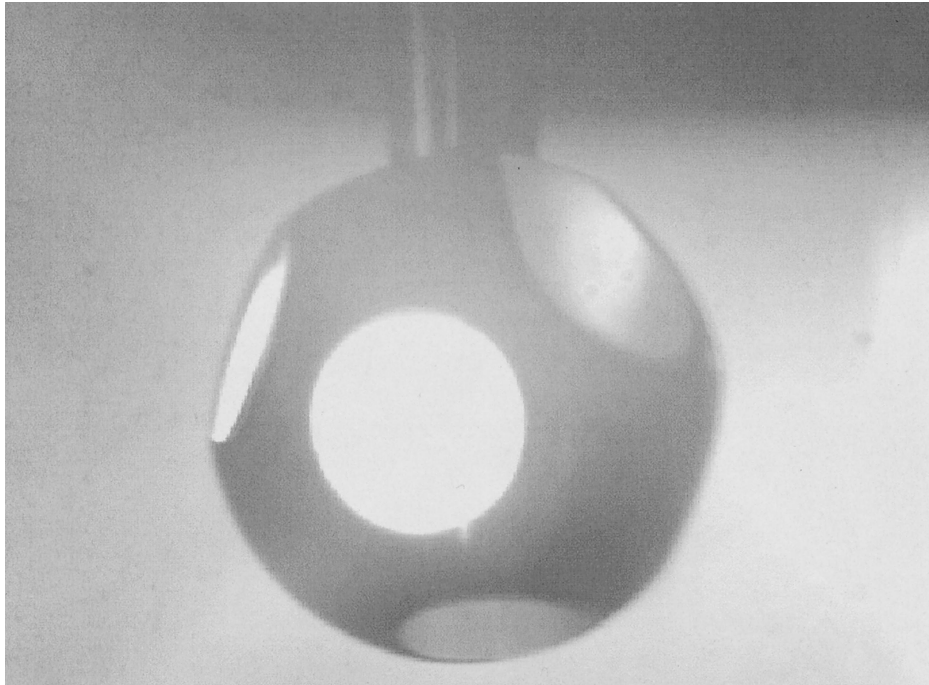
We have followed the well-known method of Fourier-transform fringe analysis,^{5,6} which we have refined in two points. One is connected to the problem of the automatic subtraction of the background, while the other deals with the problem of the removal of the heterodyning. The former may be applied to the problems involving sequences of recorded interferograms only, while the latter may be used as well

The authors are with the Institute of Physics, Bijenička 46, P.O.B. 304, 10001 Zagreb, Croatia.

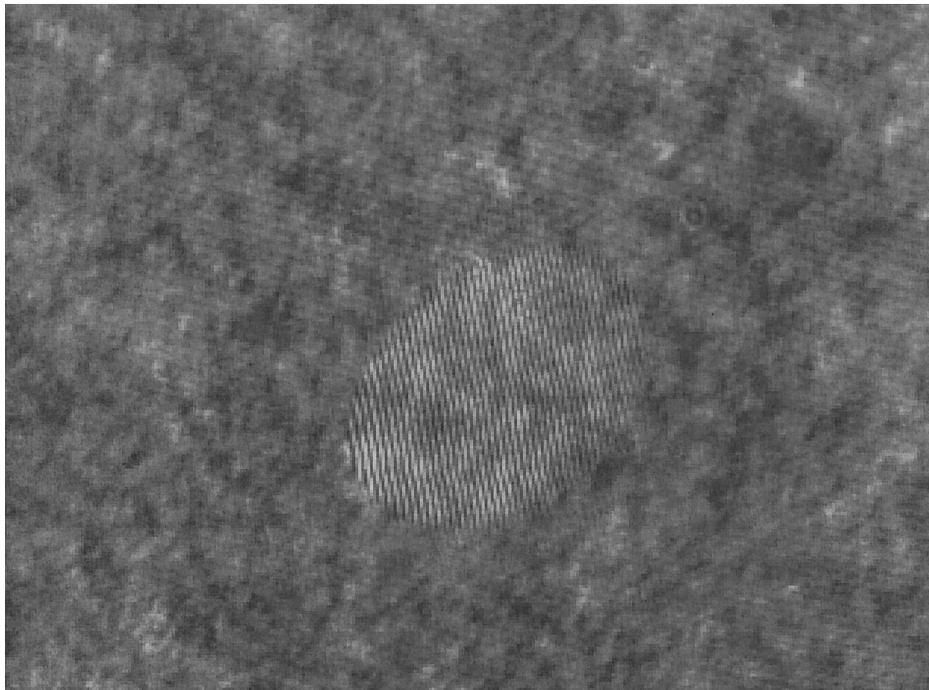
Received 6 August 2002; revised manuscript received 12 December 2002.

0003-6935/03/081477-08\$15.00/0

© 2003 Optical Society of America



(a)



(b)

Fig. 1. (a) Snapshot of a growing cuprous selenide single crystal. The bright areas correspond to atomically flat surfaces, whose outward growth has been monitored by interferometry. (b) Typical frame (320×240 pixels) recorded during the growth. The interferogram with fringe pattern (64×64 pixels) has been extracted from each frame for further analysis.

in problems in which one needs to determine the absolute phase. We first briefly describe the Fourier-transform fringe-analysis method, and then we describe our two refinements. We have tested our refinements on model interferograms, and we present the results of these tests in the last section.

2. Fringe-Pattern Analysis Method

The two-dimensional fringe-pattern is given by^{5,6}:

$$g(\mathbf{r}) = a(\mathbf{r}) + b(\mathbf{r})\cos[2\pi\mathbf{q} \cdot \mathbf{r} + \Phi(\mathbf{r})], \quad (1)$$

in which the desired information is contained in the phase field $\Phi(\mathbf{r})$, and $\mathbf{r} = (x, y)$. The functions $a(\mathbf{r})$

and $b(\mathbf{r})$, termed the amplitude and the modulation, respectively, are the functions whose spatial dependencies originate mainly from the imperfections of the measurements, because the reflecting facet is considered atomically smooth. The basic assumption of the method is that $\Phi(\mathbf{r})$, $a(\mathbf{r})$, and $b(\mathbf{r})$ are spatially slow varying functions on the scale established by the spatial-carrier frequency $\mathbf{q} = (q_x, q_y)$, which is given by the number of pixels per interference line. If this assumption is fulfilled, the Fourier spectrum contains features that are separated by vector \mathbf{q} . The standard procedure^{5,6} proceeds by extracting out, by means of some window function, one of the first-order maxima, which is centered either at \mathbf{q} or $-\mathbf{q}$, and by shifting it to the origin of the inverse space. After the inverse Fourier transform back to the real space, it is straightforward to extract the desired information, i.e., the phase field $\Phi(\mathbf{r})$. The phase difference between the two successive recorded frames, averaged over the interferogram area in real space, $\overline{\Delta\Phi}$, defines the corresponding radial displacement of the crystal facet:

$$\overline{\Delta h} = \overline{\Delta\Phi} \cdot \frac{\lambda}{4\pi} \cdot \frac{1}{\cos\left(\frac{\theta}{2}\right)}, \quad (2)$$

where λ is the wavelength of the laser beam used ($\lambda = 632.8$ nm in our experiments), and θ is the angle between the incoming laser beam and the beam reflected from the facet. The range of growth rates of the facets that we achieve in our growth experiments (1 to 10 nm/s) puts, in our experimental setup, the value of the average phase differences between two consecutive frames in the range between 0.006π and 0.3π , and we have thus been able to measure the displacements of the facet with a resolution of a few nanometers.

It should be noted that our frame-taking rate of 25 frames per s enables us to investigate, by means of laser interferometry and analysis described in this paper, the growth of crystals at very high growth rates up to 4 $\mu\text{m/s}$. This growth rate is an order of magnitude higher than the theoretical upper limit of the growth rate that may be monitored by means of the laser interferometry, cited for interferometric investigations of the growth of ^4He crystals, in which a resolution below 10 nm has been achieved for small growth rates.^{7,8}

A. Background Subtraction

Because we have been dealing with a very large number of frames (72 h of continuous frame taking during the crystal growth, at the rate of 25 frames per s), some method of automatic background subtraction is mandatory.

Our method of background subtraction is based on the idea that in a sequence of interferograms representing the growth of an object the interference lines move across the area studied. Then, by adding up a certain number of consecutive interferograms (and by normalizing this sum to the common range of gray-

level values of all interferograms, being 0–255 in our setup) one obtains an interferogram in which a larger part of the area studied is covered by the interference lines. If, by a suitable choice of the number of consecutive interferograms summed, one succeeds to fill up (approximately) the whole area studied with interference lines, one obtains an interferogram in which the interference pattern is highly (if not totally) smeared out. Because the contribution to each pixel of such interferograms comes by and large from the background, and not from the interference lines (the ratio of the weights of the two respective contributions being approximately $(n - 1)/1$, with n being the number of interferograms added), we call such an interferogram the background for these n original interferograms. (A more accurate nomenclature is the running background, because the interferograms starting from the $(n + 1)$ st have their own background determined in the same way).

The problem is then the determination of the proper number n of interferograms to be used to define such a background. The problem may be addressed by investigating the spatial Fourier spectra of the interferograms. Namely, the reduction of the interference pattern manifests itself as the decrease of the ratio of the intensities of the first-order interference peak in the Fourier domain to the zero-order peak. Because we may not expect a perfect cancellation of the interference pattern, we have established the following criterion. After each (normalized) addition of a frame, we have Fourier analyzed the sum and found the ratio of the first- to the zero-order peak intensity. As long as this ratio, as a function of the number of frames added, diminishes, the frame added contributes to the disappearing of the interference pattern. When by adding $n + 1$ frame the trend of diminishing of this ratio stops (below a certain predefined ratio, which is 0.01 in Fig. 2), we name the normalized sum of n frames the running background and subtract it from each of the first n frames contributing to it. The $(n + 1)$ st frame has then been taken as the first in the new sequence of frames that self-determine their subsequent background image. The ratio of first-order peak intensity to the zero-order peak intensity is shown in Fig. 2. By making use of the above described procedure we have been able to enhance the first- to zero-order peak intensity ratio (i.e. the signal-to-noise ratio) by more than two orders of magnitude. In Fig. 3 we present the same frame shown in Fig. 1, but with the background subtracted in the described way.

This method proves particularly useful in analyzing the interferograms for which the carrier frequency is small, i.e., for which the first-order peaks to some measure overlap with the zero-order peak. Moreover, such background subtraction enables the extraction of one of the first-order maxima to be much more straightforward, i.e., it may be done without the introduction of Gaussian (or some other) window centered at the position of the first maximum in $|g(\mathbf{q})|$. As the introduction of such a window necessarily alters the maximum one would like to extract, not

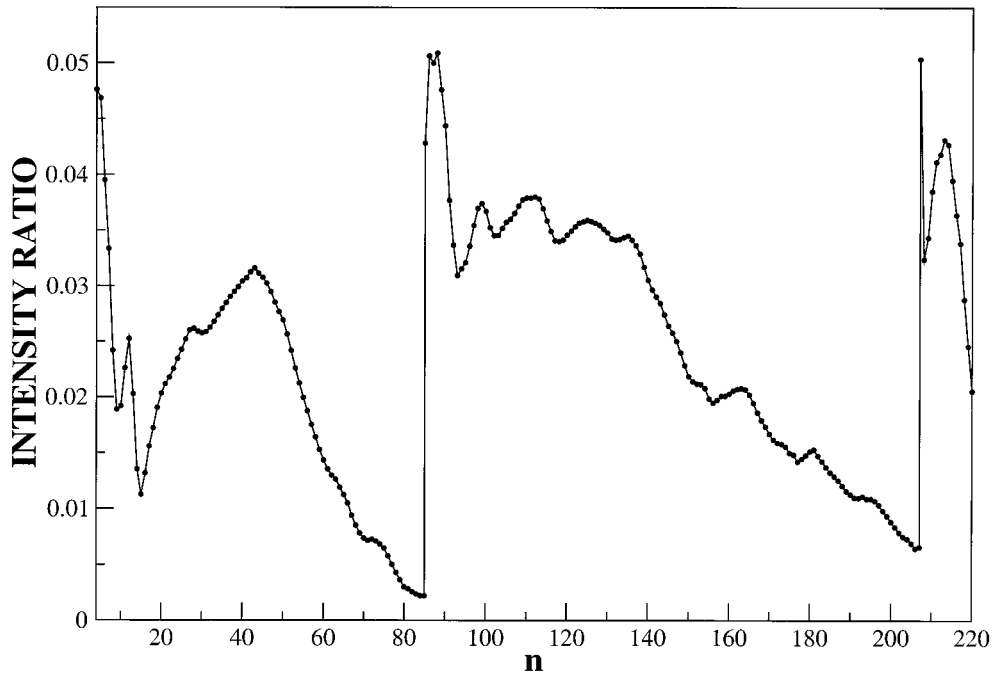


Fig. 2. Ratio of intensities of the first-order peak to the zero-order peak as a function of the index of the interferogram obtained by summing and normalizing successive interferograms. $n = 82$ concludes the first sequence, which defines the first background. The 83rd interferogram has been taken as the first one in the second sequence terminating at $n = 208$, etc.

needing this window is an additional benefit. The number of successive interferograms we have had to add to obtain good backgrounds in our crystal-growth experiments has varied from 20 to 150, depending on the growth rate and on the displacement noise induced by vibrations as well. In Section 3 we present the results of this method of background subtraction obtained on test interferograms for the most unfavourable conditions of very small carrier frequency.

B. Removal of Heterodyning

The above described procedure of shifting one of the first-order peaks into the origin of the spatial frequency domain is straightforward and exact if the carrier frequency has integer components expressed in pixels, $\mathbf{q} = \mathbf{q}_0 = (q_{0x}, q_{0y})$, i.e., this procedure is restricted to space frequencies whose components have an integer number of fringes within the area

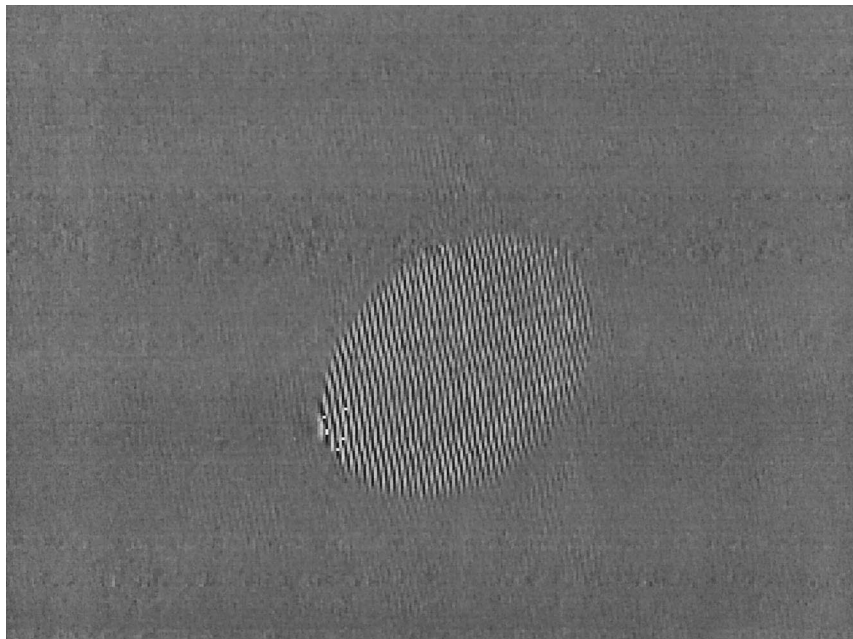


Fig. 3. Same frame as in Fig. 1(b), but with the background subtracted as described in the text.

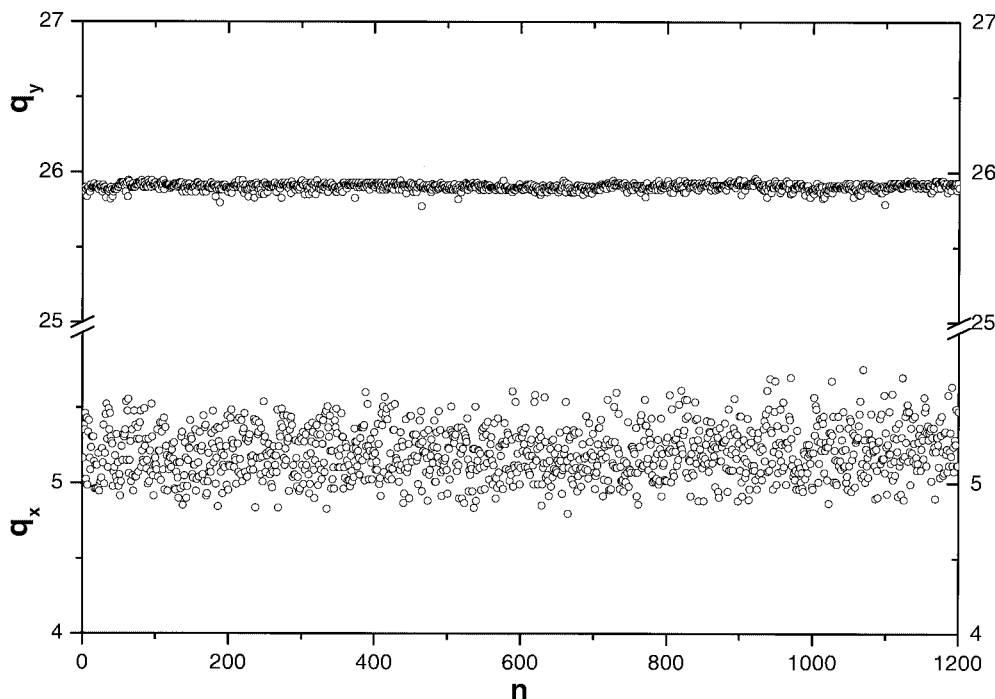


Fig. 4. Components q_x (lower panel) and q_y (upper panel) of the spatial-carrier frequency plotted versus the index of the interferograms recorded during the facet growth, and determined as described in the text.

studied. The optics of the experimental setup, as well as the above-mentioned vibrations, usually yield noninteger pixel components of \mathbf{q} , i.e., $\mathbf{q} = \mathbf{q}_0 + \delta$, where $\delta = (\delta_x, \delta_y)$, where $|\delta_x| \leq 0.5 \cdot \Delta q_x$, $|\delta_y| \leq 0.5 \cdot \Delta q_y$. Δq_x , and Δq_y measure the resolution in the spatial frequency domain. The problem then consists in finding the deviation δ of the carrier frequency from the nearest pixels in the spatial frequency domain. It is crucial for determination of the absolute values of the phase, but it has proved very important in our analysis of the crystal growth by means of phase differences between consecutive interferograms as well. In Fig. 4 we plot two components of the carrier frequency as functions of the index of the interferogram, as determined by the method we describe in Subsection 2.A. As may be seen from this figure, the values of q_x and q_y are neither integer, nor constant as functions of the interferogram index (i.e., time), as a consequence of the perturbations occurring during the growth and described in Section 1. Although the effects of such values of the components of \mathbf{q} are smaller in the case when one is interested in phase differences between two consecutive interferograms only, our aim has been the determination of these phase differences as precisely as possible to diminish the influence of the perturbations causing the variation of these components of \mathbf{q} as much as possible. By doing so we intend to obtain the dependence of the cumulative phase difference on time that would be more reliable on shorter time scales.

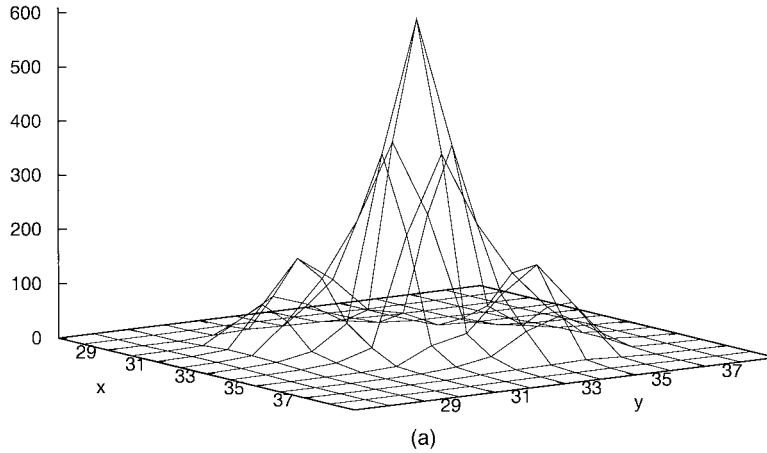
Our method proceeds by making use of the sampling theorem,⁹ which states that a continuous function, sampled at an interval Δ and a bandwidth

limited to frequencies smaller than the Nyquist critical frequency $1/(2\Delta)$ is completely determined by its samples. We have applied this theorem in the spatial frequency domain, to the amplitude of the Fourier transform $|g(\mathbf{q})|$, $\mathbf{q} = (q_x, q_y)$, which is a well-behaved function in the frequency domain. Explicitly, one has the following interpolation formula:

$$|g(q_x, q_y)| = \sum_{m,n} |g_{m,n}| \frac{\sin\left[\pi\left(\frac{q_x}{\Delta q_x} - m\right)\right]}{\pi\left(\frac{q_x}{\Delta q_x} - m\right)} \cdot \frac{\sin\left[\pi\left(\frac{q_y}{\Delta q_y} - n\right)\right]}{\pi\left(\frac{q_y}{\Delta q_y} - n\right)}, \quad (3)$$

where $g_{m,n}$ stands for $g(q_x = m \cdot \Delta q_x, q_y = n \cdot \Delta q_y)$. By making use of this formula, one may calculate $|g(\mathbf{q})|$ on the arbitrary dense subgrid defined around the integer-pixel point \mathbf{q}_0 limited by $|\delta_x| \leq 0.5 \cdot \Delta q_x$, $|\delta_y| \leq 0.5 \cdot \Delta q_y$, and obtain its values to any chosen subpixel accuracy. The maximum of these values defines δ , i.e., the deviation of the carrier frequency components from the integer pixel values. Now we proceed by shifting the chosen first-order maximum to the origin of the spatial frequency domain by the integer values \mathbf{q}_0 , and upon the inverse-Fourier transformation we obtain $G_0(\mathbf{r})$, which defines the uncorrected phase field $\Phi_0(\mathbf{r})$. By expanding $g(\mathbf{q})$ (which is, owing to the noise contributions a and b , a continuous function around \mathbf{q}) in Taylor series around \mathbf{q}_0 , and by performing the inverse-Fourier

FOURIER SPECTRUM



FOURIER SPECTRUM

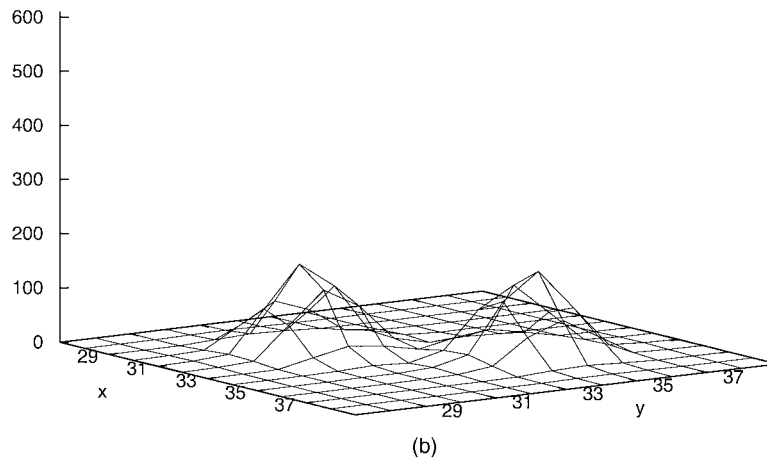


Fig. 5. Fourier transform of an interferogram defined by Eqs. (1) and (6) with parameters as given in text: (a) without the subtraction of the background; (b) with the background subtracted. The point with coordinates (in pixels) $x = 33$ and $y = 33$ represents the $\mathbf{q} = \mathbf{0}$ point of the inverse space.

transform, one obtains, as expected, for the correction arising from the subpixel correction δ to \mathbf{r} :

$$\Delta G(\mathbf{r}) = \exp(i\delta \cdot \mathbf{r}), \quad (4)$$

and the corrected value of the inverse transform becomes

$$G(\mathbf{r}) = G_0(\mathbf{r})\exp(i\delta \cdot \mathbf{r}). \quad (5)$$

It is now straightforward to calculate from $G(\mathbf{r})$ the corrected phase field $\Phi(\mathbf{r})$.

We have tested the above-described procedure on test interferograms involving predefined noninteger components of the carrier frequency, and obtained the exact noninteger value of the carrier frequency within any selected accuracy. It may be noted that our method diminishes the influence of the limits that the resolution of the camera imposes on frames recorded.

3. Tests

In this section we present the results of our methods of background subtraction in the highly unfavorable case of a small number of interference lines within the interferogram area studied, i.e., in the case of small spatial carrier frequency \mathbf{q} and of the removal of heterodyning as described earlier in the text. Our model interferograms have been given by Eq. (1). The functions $a(\mathbf{r})$ and $b(\mathbf{r})$, simulating the amplitude and the modulation of perturbed interferograms, have been taken from Ref. 10:

$$\begin{aligned} a(\mathbf{r}) &= n_0\rho - b_0(2y^3 - 4y + 2)(2x^2 - 2x) \\ b(\mathbf{r}) &= [1 - m_0(y^2 - 2y + 1)] \\ &\quad \times [1 - m_0(4x^2 - 4x + 1)]. \end{aligned} \quad (6)$$

Here the coordinates x and y are normalized to $0 \leq x, y \leq 1$, and ρ is a random number distributed within

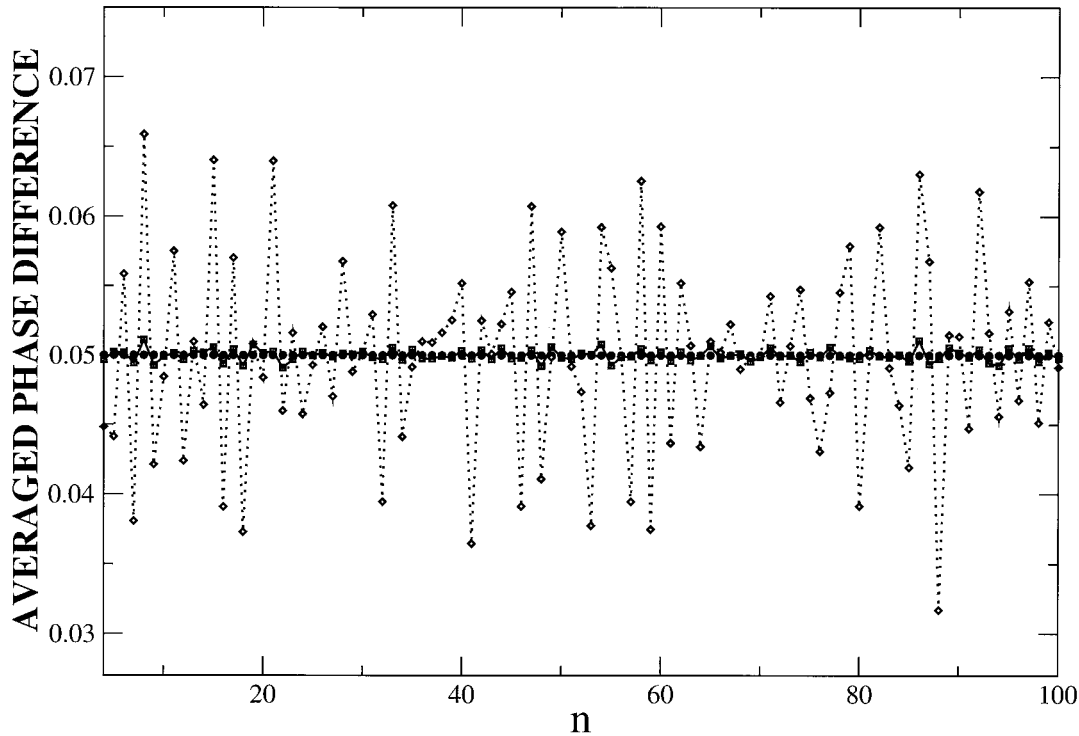


Fig. 6. Filled circles: chosen value of the averaged phase field difference between consecutive interferograms. Dotted curve with open diamonds: calculated values of the averaged phase field difference without taking account of noninteger and varying values of spatial-carrier frequency. Solid curve and open squares: calculated values of the averaged phase field difference with all of the components of the spatial-carrier frequency removed as described in the text.

the range between -1 and 1 . The parameters n_0 , b_0 , and m_0 are the amplitudes of the perturbative components expressed as percentages of the perturbation-free amplitude of fringes. The noninteger components of the spatial-carrier frequency have been randomized in the intervals between $-0.25\Delta q_i$ and $0.25\Delta q_i$, $i = (x, y)$, around the basic carrier frequency to simulate our real situation as depicted in Fig. 4.

We have constructed a series of interferograms given by Eqs. (1) and (6). The values of the parameters n_0 , b_0 , and m_0 have been set equal, and have been varied in our test up to the value as high as 0.5 , i.e., the level of spurious components of the interference patterns¹⁰ has been set up to 50% of the unperturbed amplitude of fringes. We have incorporated in these parameters, for each interferogram in the series, a small random contribution as well, to simulate the effects of short time vibrations that have influenced our experiments. Because we wanted to simulate our real interferograms describing the growth of the crystal facets, we have modeled the phase field in a way that it had, when averaged over the area of the interferogram, a linear increasing trend in cumulative phase differences. Moreover, each phase field has been modeled by a low spatial-frequency sinusoidal field. In Fig. 5(a) we plot the Fourier transform of a typical interferogram taken from the series described above. The basic values of the components of the spatial-carrier frequency have

been $q_x = 1.78\Delta q_x$ and $q_y = 1.87\Delta q_y$, and these values have been randomized for the reason described above. The level of spurious components of the interference patterns has been 50% of the unperturbed amplitude of fringes. In Fig. 5(b) we plot the Fourier transform of the same interferogram but with the background subtracted by the procedure discussed. One may see that our procedure successfully reduces the background, i.e., the zero-order peak, to the very low level, even in such an unfavorable case in which the zero-order peak overlaps significantly with the first-order maxima in which the desired information is stored, and with such a high level of perturbation of interference patterns. We stress once again that, as described earlier, our background changes, and that the entire sequence of recorded interferograms is in this way divided into sections, and each of these sections has its own best background.

In Fig. 6 we show a typical result of our tests of our method of the removing of heterodyning. We constructed a series of interferograms as described above, by means of Eqs. (1) and (6). To concentrate solely on the problem of the removing of heterodyning, the only parameters varying from interferogram to interferogram have been the values of spatial-carrier frequency components and q_y . These values have been randomized within the intervals between $-0.25\Delta q_i$ and $0.25\Delta q_i$, $i = (x, y)$, around their basic values to simulate our real situation (cf. Fig. 4). The average value of the phase field for all interferograms

has been set to 0.05 in a test the results of which are shown in Fig. 6. It may be seen that our procedure yields significantly better results as compared with the calculations obtained without the correction dealing with noninteger (in pixels) values of the carrier-frequency components, which vary between successive interferograms. We note that such a correction is essential when one is interested in absolute values of the phase field.

4. Conclusion

We conclude that our refinement of the Fourier method of analysis of interference fringes may be very useful in analyzing long sequences of interferograms, especially when one has just a few interference lines within the data window. We stress that the described procedure enables us to extract the difference in phase field of successive interferograms with high accuracy. Such phase-field differences still carry a contribution arising from slow mechanical vibrations (the corresponding time scale being larger than 10 s) of the experimental setup. However, these contributions may then be analyzed and (at least partially) removed on the basis of the whole series of interferograms recorded, as stated in Section 1. The preliminary results of our analysis of the growth of cuprous selenide single crystals includes both the method presented in this paper and the method of dealing with the above-mentioned slow mechanical vibrations, which has been presented elsewhere.³ Detailed results will be presented in a future paper. It should be noted that our analysis

may be implemented in real-time one only in the case of one-dimensional interferograms.

References

1. Z. Vučić and J. Gladić, "Growth rate of equilibrium-like-shaped single crystals of superionic conductor cuprous selenide," *J. Cryst. Growth* **205**, 136–152 (1999).
2. Z. Vučić and J. Gladić, "Shape relaxation during equilibrium-like growth of spherical cuprous selenide single crystals," *Fizika A* **9**, 9–26 (2000).
3. Z. Vučić, J. Gladić, D. Lovrić, S. Mitrović, M. Milas, and N. Demoli, "Mechanism of growth of equilibrium-like-shaped cuprous selenide single crystals," Third scientific meeting of the Croatian Physical Society, Book of Abstracts, 113 (2001).
4. G. C. Brown and R. J. Pryputniewicz, "Holographic microscope for measuring displacements of vibrating microbeams using time-averaged, electro-optic holography," *Opt. Eng.* **37**, 1398–1405 (1998).
5. M. Takeda, H. Ina, and S. Kobayashi, "Fourier-transform method of fringe-pattern analysis for computer-based topography and interferometry," *J. Opt. Soc. Am.* **72**, 156–160 (1981).
6. W. W. Macy, Jr., "Two-dimensional fringe-pattern analysis," *Appl. Opt.* **22**, 3898–3901 (1983).
7. F. Gallet, S. Balibar, and E. Rolley, "The roughening transition of crystal surfaces. II. Experiments on static and dynamic properties near the first roughening transition of hcp 4He," *J. Phys. (France)* **48**, 369–377 (1987).
8. J. P. Ruutu, P. J. Hakonen, A. V. Babkin, A. Yu. Parshin, and G. Tvalashvili, "Growth of ⁴He-Crystals at mK-Temperatures," *J. Low Temp. Phys.* **112**, 117–164 (1998).
9. See for example W. H. Press, S. A. Teukolsky, W. T. Vetterling, and B. P. Flannery, "Numerical Recipes," (Cambridge University U.K., 1992), Chap. 12.
10. D. J. Bone, H.-A. Bachor, and R. J. Sabdeman, "Fringe-pattern analysis using a 2-D Fourier transform," *Appl. Opt.* **25**, 1653–1660 (1986).